Exp Fluids (2009) 46:549–558
DOI 10.1007/s00348-008-0580-7

RESEARCH ARTICLE

Influence of surfactant upon air entrainment hysteresis in curtain coating

J. O. Marston · V. Hawkins · S. P. Decent · M. J. H. Simmons

Received: 16 May 2008 / Revised: 1 July 2008 / Accepted: 7 October 2008 / Published online: 5 November 2008

Abstract The onset of air entrainment for curtain coating onto a pre-wetted substrate was studied experimentally in similar parameter regimes to commercial coating ($Re = \rho Q/\mu = O(1)$, $We = \rho Q u_c/\sigma = O(10)$, $Ca = \mu U/\sigma = O(1)$). Impingement speed and viscosity were previously shown to be critical parameters in correlating air entrainment data with three qualitatively different regimes of *hydrodynamic assist* identified (Marston et al. in Exp Fluids 42(3):483–488, 2007a). The interaction of the impinging curtain with the pre-existing film also led to a significant hysteretic effect throughout the flow rate-substrate speed parameter space. For the first time, results considering the influence of surfactants are presented in attempt to elucidate the relative importance of surface tension in this inertia-dominated system. The results show quantitative and qualitative differences to previous results with much more complex hysteretic behaviour which has only been reported previously for rough surfaces.

List of symbols

g	gravitational constant (ms^{-2})
h	curtain height (cm)
Q	curtain flow rate ($cm^2\ s^{-1}$)
U	substrate speed (ms^{-1})
u_c	curtain impingement speed (ms^{-1})
c	film thickness (m)
P_l	pressure load (Nm^{-2})
t_r	curtain residence time (s)
w	curtain width (μm)

Greek letters

μ	viscosity (mPa s)
σ	surface tension (m Nm^{-1})
ρ	density (kg m^{-3})

Subscripts

max maximum

1 Introduction

High speed coating processes involving the deposition of a liquid onto a solid moving at speeds of $O(10)$ ms^{-1} are central to many industries in the final stages of production of photographic films and papers, protective finishes and adhesive layers. The fundamental aim of such processes is the rapid production of defect-free coatings. To achieve this aim requires an understanding of the mechanisms which can lead to defects and non-uniformities. Such defects can often be attributed to two stages in the production: coating and drying. In the case of the former, which has been the focus of many previous experimental and theoretical studies, the defects can arise from instabilities originating from the contact line where the coating liquid first meets the target surface. In this case, instability

J. O. Marston · V. Hawkins · M. J. H. Simmons
School of Chemical Engineering, University of Birmingham, Edgbaston, Birmingham, UK

Present Address:
J. O. Marston (✉)
A-STAR Institute of Chemical and Engineering Sciences, 1 Pesek Road, Jurong Island, Singapore 627833, Singapore
e-mail: jeremy_marston@ices.a-star.edu.sg

S. P. Decent
School of Mathematics, University of Birmingham, Edgbaston, Birmingham, UK

can be characterised by the entrainment of air bubbles into the coated film (synonymous with dynamic wetting failure). The method of application of the liquid will be governed by the nature of the product, required quality of the coating and the physical and chemical properties of both the solid and liquid in question. One particular method which has proven itself beneficial for some manufacturers is the curtain coating method; a gravity-driven inertia-dominated method where a thin liquid sheet (typically $O(10^{-5}-10^{-4})$ m) falls vertically onto a substrate passed underneath. The specific feature that makes curtain coating attractive to manufacturers is the ability to coat at speeds typically $O(1000)$ m/min, which is attributed to the inertial pressure load at the point of impingement suppressing the entrainment of air at the contact line. This feature, termed *hydrodynamic assist*, was first reported in the literature by Blake et al. (1994) and has since been examined in a number of curtain and jet coating geometries (Blake et al. 1999, 2004; Clarke 2002; Marston et al. 2006a, b, 2007a, b; Yamamura et al. 1999, 2006).

Blake et al. (1994) reported that the substrate speed at the onset of air entrainment phenomenon, observed by increasing the substrate speed for fixed curtain flow rates, was dependent on the flow rate. In addition to this, they also reported that the air entrainment was subject to hysteresis, i.e. the speed at which air entrainment ceases when the substrate speed is decreased is not the same as that for the onset. These observations were made for smooth substrates and non-Newtonian fluids. They concluded the following correlation for air entrainment data:

$$U_{\max} = 8.09 u_c^{0.81} \mu^{-0.19} \quad (1)$$

where $U_{\max}$ is the substrate speed at the onset of air entrainment, $u_c = \sqrt{2gh}$ is the curtain impingement speed, where g is the acceleration due to gravity, h is the curtain height and μ is the liquid dynamic viscosity. The effect of initial curtain speed for a die geometry is negligible once the curtain height reaches a few centimetres as shown by Marston (2008), thus the free-fall approximation as used by Blake et al. (1994, 1999, 2004) is justified.

Marston et al. (2006a, b, 2007a, b) performed experiments in a curtain coating geometry onto a pre-wetted surface to show, for Newtonian fluids, not only that the substrate speed for air entrainment was flow-rate dependent, but that it is subject to hysteresis and in some cases, non-unique. The curtain impingement speed and viscosity were shown to be critical parameters and, by careful selection, three distinct, increasingly intense modes of assist were observed. This hysteresis, which becomes most significant in the more intense modes of assist, was attributed partly to the dynamical interaction between the curtain and the pre-wet film, which essentially provides a lubrication for the impinging curtain and may induce non-linear behaviour. For the more intense modes of assist, three-dimensional heels formed at the onset of instability are also likely to contribute.

The observations of air entrainment were made by a variety of examinations of the flow rate—substrate speed parameter space; firstly by fixing the flow rate and increasing substrate speed (*horizontal analysis*); Secondly by fixing substrate speed and increasing flow rate (*vertical analysis*); And thirdly by a combination (*path-dependent analysis*). By performing these different analyses, the parameter space was shown to exhibit areas where the flow was always stable, always unstable, subject to hysteresis and metastable.

In this paper, experimental observations of air entrainment hysteresis in curtain coating of Newtonian fluids are extended to examine the influence of surface tension by the addition of surfactant into the coating fluids. The results are compared to previously obtained results showing qualitative and quantitative differences. It is found that the addition of surfactant leads to multiple regions of stability for a given flow rate. Although inertial effects are clearly still significant, the new hysteresis observations can only be attributed to surfactant-induced instability.

2 Experimental

A schematic of the pilot-scale curtain coating facility is shown in Fig. 1. The continuous substrate was provided by a rotating stainless steel wheel, with a diameter of 0.45 m and a width of 0.06 m. The surface was highly polished so that the average surface deviation (R_a) was 52 nm ± 2 nm as measured by an Atomic Force Microscope (AFM). The wheel was driven by a 0.55 kW motor with inverter feedback control (Eurotherm 690+ series) producing a range of substrate speeds from 0.15 to 2.3 ms^{-1}.

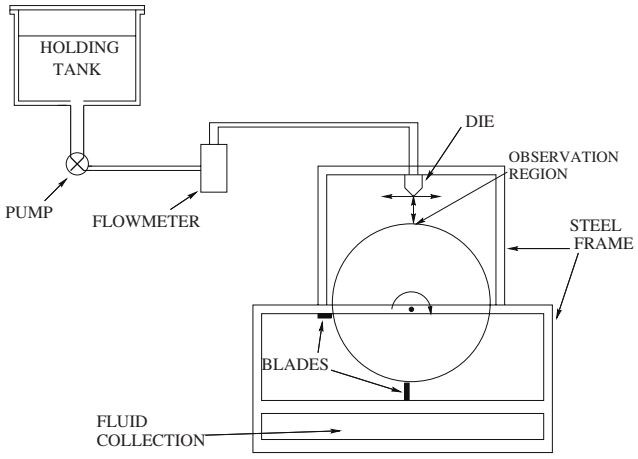

Fig. 1 Schematic of the curtain coating apparatus used

The fluids used were 85 and 90% aqueous glycerol solutions (Croda, UK). The fluid dynamic viscosities were measured using a Contraves Rheomat-30 viscometer equipped with a cup and bob attachment. Measurements of these properties were made over a range of temperatures enabling the correct values to be used given the temperature of the fluids used within the facility. Due to ambient laboratory conditions, fluid temperatures varied from 19 to 24°C, however, the temperature of the fluids used remained constant over the duration of a single experiment.

Static surface tension measurements, as measured by a du Nouy ring tensiometer, are sufficient for aqueous glycerol solutions in the absence of surfactant since the relaxation of glycerol molecules is many orders of magnitude smaller than the residence time in the curtain (Lin and Roberts 1981) and, as such, the curtain is considered to be in thermodynamic equilibrium.

However, in this study, to examine the influence of surface tension, surfactant was introduced into the water-glycerol mixtures at increasing concentrations (0.1, 0.2 and $0.3\%_{w/w}$). The surfactant used was SDS (Sodium Dodecyl Sulphate) for its ability to significantly reduce the surface tension of aqueous solutions using low concentrations. Measurement of the surface tension properties of surfactant in the glycerol solutions at the concentrations used is complicated by viscous effects (Fainerman et al. 1993, 2004). As such, for a first approximation the value of the surface tension is derived by equating the curtain residence time $t_r = \sqrt{2h/g}$ with a specific bubble lifetime for the measurements made with a 50% glycerol solution ($\mu = 8.4$ mPa s) using a T60 bubble pressure tensiometer (SITA Messtechnik GmbH, Germany). Plots of surface tension against surface age for this fluid are shown in Fig. 2 for 0.1, 0.2 and 0.3% SDS.

The properties for the fluids used in this study, at the temperature of the experiments, are given in Table 1.

After the addition of surfactant, the rheology of the fluids was tested and no non-Newtonian behaviour was observed. The viscosity was also checked and found to be independent on surfactant concentration.

The fluids were supplied to a four-slot die of width 0.09 m (based on a design by Kodak Ltd., UK) using a high accuracy gear pump (Series 200, Liquiflo, USA). Flow rates, measured by an electromagnetic flow meter (IFM5020K/D, Krohne, Germany), ranging from 1 to 10 cm^2s^{-1} (defined per unit width of curtain) were possible. The flow-meter was calibrated by weighing collected fluid over certain time intervals and flow rates and was determined to be accurate to within 3.5%. The integrity of the falling curtain was maintained by using copper or stainless steel wires of 1.6 mm diameter as edge guides (for

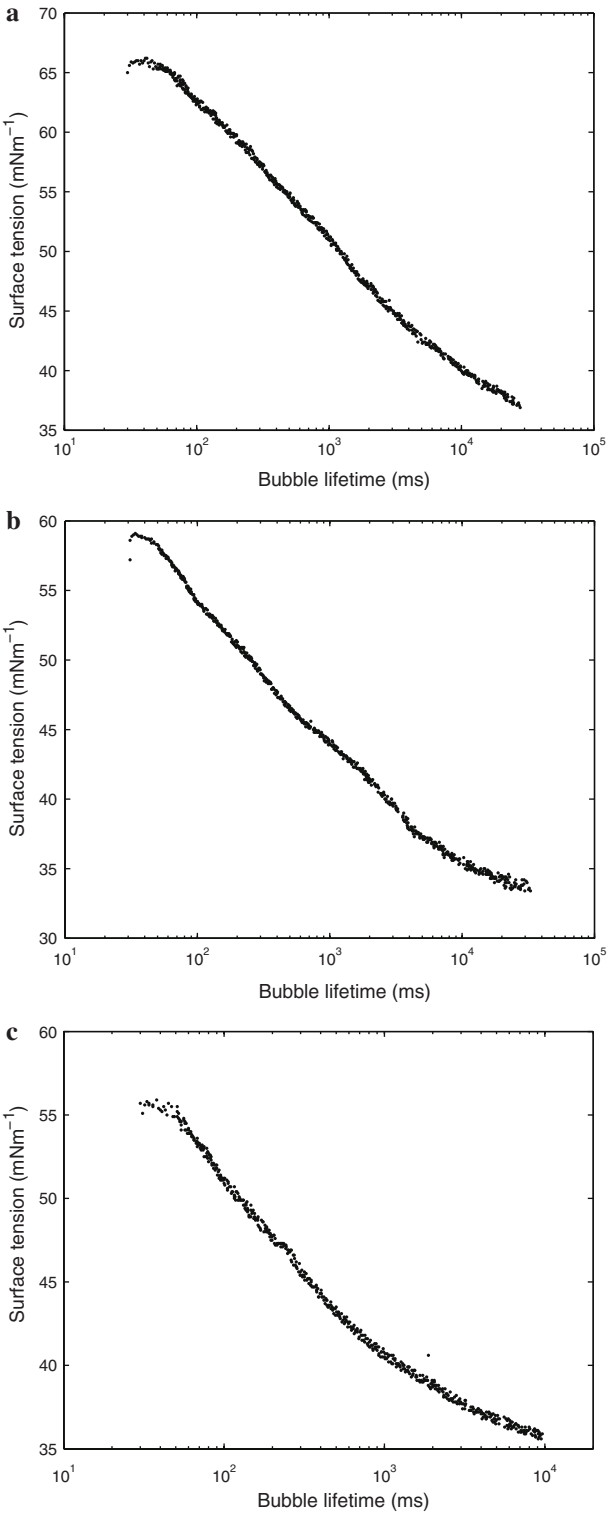

Fig. 2 Plot of surface tension against bubble lifetime (effective surface age) for **a** 0.1% SDS, **b** 0.2% SDS and **c** 0.3% SDS in 50% glycerol solutions ($\mu = 8.4$ mPa s). Approximate values of surface tension can be extracted by reading off the graph at bubble lifetimes corresponding to curtain residence times

Table 1 Properties of glycerol–water mixtures with surfactant at laboratory temperature of experiments (approximate concentrations % v/v)

Glycerol	SDS	ρ	μ	σ_s	$\sigma_{t1}/\sigma_{t2}/\sigma_{t3}$
85	0	1,261	117	67	NA
85	0.1	1,261	129	36.9	64/62/60.8
85	0.2	1,261	114	33.4	56.3/53.7/52.4
85	0.3	1,261	119	35.6	53.2/50.1/48.9
90	0	1,269	215	66.5	NA
90	0.3	1,269	267	35.6	53.2/50.1/48.9

The surface tensions stated for the solutions with SDS (approximate concentrations % w/w) are the values measured in 50% glycerol-water mixtures (from Fig. 2) equating bubble lifetime to given curtain residence times; $t_1 = 0.073$ s, $t_2 = 0.116$ s, $t_3 = 0.147$ s

low viscosity fluids) and perspex windows (for high viscosity fluids).

Removal of the bulk of the liquid film from the solid substrate post coating was performed using a series of double-v headed urethane 'squeegee' blades. The blades were mounted between steel plates, bolted to the outer frame and pressed tightly against the surface. These blades remove most, but not all of the liquid, leaving a residual film. The coating surface was therefore pre-wetted and estimates of the thickness of the residual film were produced by placing absorbent material onto the rotating wheel before the coating die for 10 revolutions during the coating process. Results for the thickness of the residual film indicate that it is at least of the order of 10^{-7}–10^{-6} m (Marston et al. 2006a, b), sufficient to eliminate any surface roughness effects (Clarke 2002).

The precise thickness of the residual film could not be preset at a specific value using this method, however, repeatability of both the onset speeds and the thicknesses of the film at various points in the parameter space of interest indicate that the thickness is independent of curtain flow rate and does not vary dynamically throughout the course of any experiments (Marston et al. 2006a), i.e. c is not a dynamic variable. Hence the hysteresis is owed to true non-linear effects of the flow.

Measurements of the substrate (wheel) speed at the onset of air entrainment were made for each of the fluids given in Table 1 at various (arbitrary) curtain heights of 2.6, 6.6 and 10.7 cm to permit study of the influence of surfactant for increasingly intense hydrodynamic effects; an increase in curtain height leads to an increase in curtain impingement velocity ($u_c = \sqrt{2gh}$), which in turn leads to a decrease in curtain width ($w = Q/u_c$). The onset of air entrainment was obtained by increasing the substrate speed, U, at constant curtain flow rate, Q, until wetting (coating) failure and entrainment of air bubbles was observed with the naked eye. In true dynamic wetting problems, dynamic wetting failure—where the wetting line ceases to advance normal to itself and adopts a sawtooth configuration—can occur before the onset of air entrainment. Equally, when the surface is pre-wetted, the liquid may fail to coat the surface before air entrainment occurs, i.e. the apparent contact line may destabilise without evidence of air bubbles. However, these two points could not be distinguished in these experiments, as also observed by Cohu and Benkreira (1998) for dip coating.

To repeat measurements, the substrate speed was decreased from the onset of air entrainment until clearance, where no bubbles were seen and stable coating resumed. There was a notable difference between the speed at the onset and clearance of air entrainment in some cases which produces regions of hysteresis.

For the case of glycerol solutions with surfactant, the hysteresis becomes significantly more complex with multiple onset and clearance speeds obtained by both increasing and decreasing substrate speed for fixed flow rates.

The procedure was then repeated for higher values of Q until the substrate speed at the onset of air entrainment was no longer a function of Q. Each data point was repeated a minimum of three times and the observed variation was less than 3%.

3 Results and discussion

3.1 Surfactant-free solution

Figure 3 shows a typical air entrainment curve for a low viscosity ($\mu = 117$ mPa s) glycerol solution for a curtain height $h = 6.6$ cm. The data points were generated by setting Q and increasing U until air entrainment occurred ('Onset') then decreasing U until stable coating resumed ('Clearance'). To the right of the 'onset' data points, the

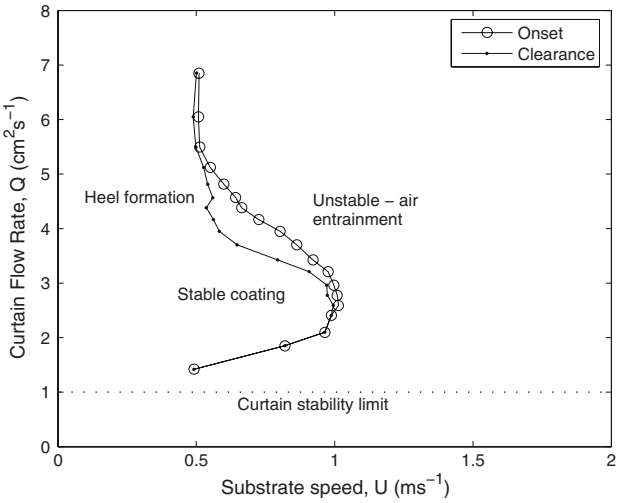

Fig. 3 Air entrainment curve marking onset and clearance speeds for a 117 mPa s glycerol solution with a curtain height of 6.6 cm

flow downstream of the curtain is unstable with air bubbles and to the left of the 'clearance' data points, the flow is stable. For high flow rates ($Q > 4$ cm^2 s^{-1}), a liquid 'heel' forms upstream of the curtain. For low flow rates ($Q < 1$ cm^2 s^{-1}), the curtain flow is dominated by surface effects and may neck-in laterally or rupture into threads. The curve is typical of coating windows observed using the curtain coating method (Blake et al. 1994, 2004; Marston et al. 2006a, b, 2007a, b).

The main features are the maximum coating speed $U_{\max} = 1.01$ ms^{-1} at the corresponding flow rate $Q_{\max} = 2.59$ cm^2 s^{-1}, when the contact line is understood to be directly beneath the impinging curtain (Blake et al. 1994; Yamamura et al. 1999), and the flow-field independent speed $U_i = 0.51$ ms^{-1} for flow rates $Q_i \gtrsim 5.5$ cm^2 s^{-1}. For $Q \leq Q_{\max}$ and $Q \geq Q_i$, there is negligible hysteresis, that is, the speeds at the onset and clearance of air entrainment largely coincide. For $Q_{\max} < Q < Q_i$, however, the two boundaries appear to diverge and substantial hysteresis is observed. In the region formed by these two boundaries, stability will depend upon the route taken through the parameter space (Marston et al. 2006b).

The data here conforms to previously derived correlations for the onset of air entrainment (Marston et al. 2006a) where the constants have been modified due to an expanded data set

$$U_{\max} = 7.65 u_c \mu^{-0.45}, \tag{2}$$

for the maximum speed and

$$U_i = 19.7 \mu^{-0.75}, \quad \mu \leq 365, \tag{3}$$

for the flow-field independent speed. These equations yield predictions of 1.02 and 0.55 ms^{-1}, respectively for the fluid used in Fig. 3.

Figure 4 shows the equivalent curves for curtain heights of 2.6 and 10.7 cm. The influence of the hydrodynamics upon the maximum attainable coating speed are evident. Increasing the curtain height increases the inertial pressure load, $P_l \sim \frac{\rho u_c^2}{4}$, which is the mechanism that has been linked to the higher coating speeds in the curtain coating geometry (Blake et al. 1994; Clarke 2002; Marston et al. 2007a). As such, increasing curtain height is expected to lead to higher maximum substrate speeds at the onset of air entrainment.

The maximum speeds here are 0.69 and 1.24 ms^{-1}, respectively, again in reasonable agreement with Eq. 2. Note also that $Q_{\max}$ decreases for increasing curtain height and that the hysteretic effect becomes increasingly profound.

3.2 Surfactant-filled solution

The above analysis was replicated for a similar viscosity solution ($\mu = 119$ mPa s) with 0.3% SDS added. Figure 5 shows a comparison between the curve for the onset of air entrainment with and without surfactant at the lowest curtain height, $h = 2.6$ cm, to minimise hydrodynamic effects. Note that the clearance curve is not shown due to negligible hysteretic effects.

It is immediately clear that the presence of surfactant in the solution is having a profound influence on the stability of the contact line. The maximum substrate speed for the surfactant solution $U_{\max} = 0.23$ ms^{-1} is a factor of 3 smaller than the surfactant-free solution. In addition, the speed at the onset of air entrainment is now only weakly dependent on the flow rate. That is, there is minimal *hydrodynamic assist* and the stability appears to be

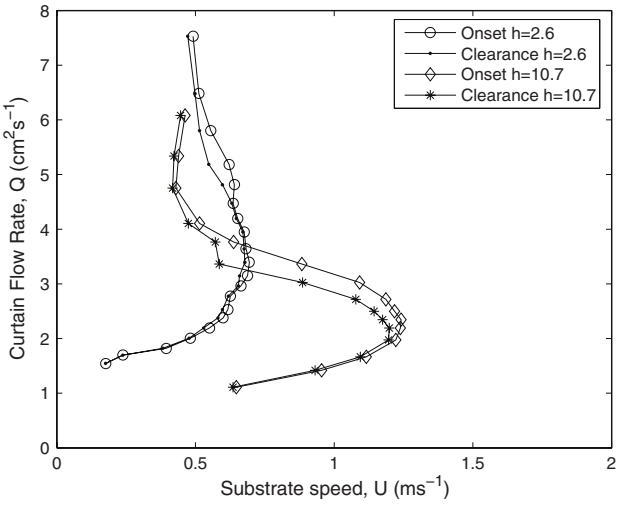

Fig. 4 Air entrainment curves marking onset and clearance speeds for a 117 mPa s glycerol solution with curtain heights of 2.6 and 10.7 cm

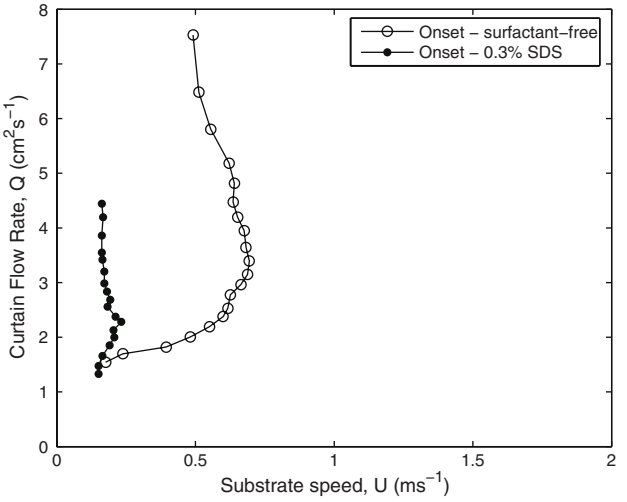

Fig. 5 Onset of air entrainment for a 119 mPa s glycerol solution with 0.3% SDS. $h = 2.6$ cm. Also shown is the original curve for the surfactant-free solution ($\mu = 117$ mPa s)

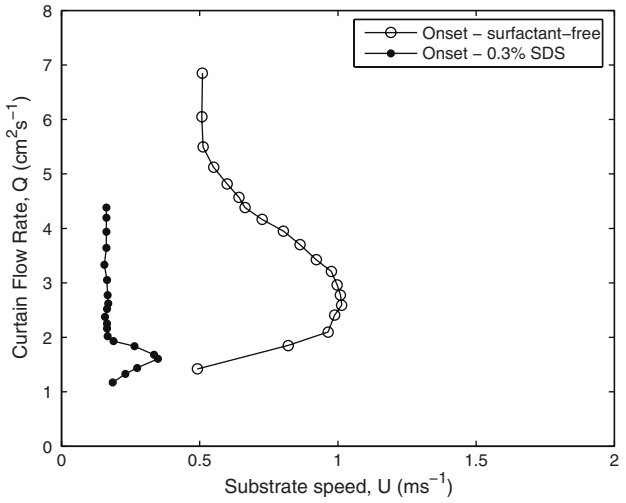

Fig. 6 Onset of air entrainment for a 119 mPa s glycerol solution with 0.3% SDS. $h = 6.6$ cm. Also shown is the original curve for the surfactant-free solution ($\mu = 117$ mPa s)

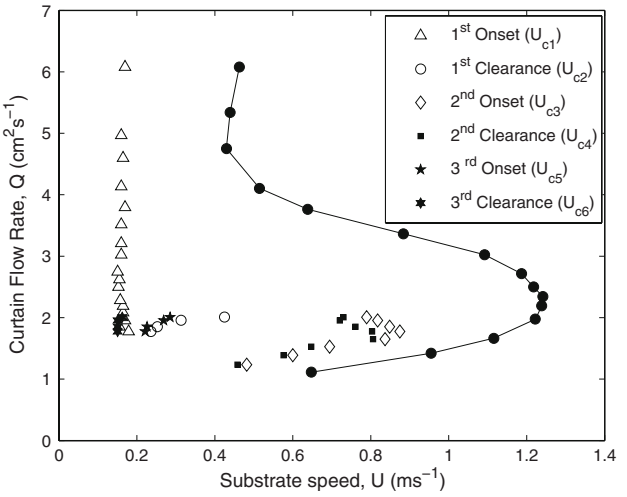

Fig. 7 Onset of air entrainment for a 119 mPa s glycerol solution with 0.3% SDS. $h = 10.7$ cm. Also shown is the original curve (*filled circles*) for the surfactant-free solution ($\mu = 117$ mPa s)

dominated by surface tension. If the value of surface tension indicated in Table 1, $\sigma_{t1} = 53.2$ m Nm^{-1} is taken, then it is clear that the air entrainment phenomena is strongly dependent on surface tension (a fact already well established for various other coating methods) for this geometry. For the solution containing surfactant, $U_i \approx 0.15$ ms^{-1} which is well below that predicted by Eq. 3 (0.55 ms^{-1})

Figure 6 plots the equivalent data for a curtain height $h = 6.6$ cm. Again, there is minimal hysteresis and so the clearance curve is not shown, and a near three-fold decrease in maximum speed is observed for the surfactant solution with $U_{\max} = 0.34$ ms^{-1}. For this curtain height, there is a small degree of hydrodynamic assist (flow rate dependence) but it is restricted to the range 1 cm^2 s^{-1} $< Q <$ 2 cm^2 s^{-1}.

For the two curtain heights in Figs. 5 and 6 ($h = 2.6$ and 6.6 cm) it can be seen that the reduction of surface tension leads to a large decrease in the degree of hydrodynamic assist of the coating process and negligible hysteresis. In contrast, Fig. 7 shows data obtained for a curtain height $h = 10.7$ cm where hydrodynamic effects are only slightly reduced and there is a much more complex hysteresis. The data obtained here requires more explanation. For $Q <$ 1.7 cm^2 s^{-1}, there is regular hydrodynamic assist with a maximum substrate speed $U_{\max} = 0.87$ ms^{-1}. For $Q >$ 2.1 cm^2 s^{-1}, the flow-field independent regime is reached with $U_i = 0.16$ ms^{-1}, as with Figs. 5 and 6. The transition between the hydrodynamic regime and the flow-field independent regime, i.e. $Q_{\max} < Q < Q_i$, is however substantially more complex than previous experiments. To describe the phenomenon here, consider the case for $Q = 2$ cm^2 s^{-1}. The first critical speed is that which corresponds to the first observation of instability by increasing U from very low values, $U_{c1} = 0.16$ ms^{-1}. By increasing U from this instability, the contact line subsequently stabilises at $U_{c2} = 0.42$ ms^{-1} with no evidence of air entrainment. Further increase in U leads to the usually defined maximum speed at the onset of air entrainment $U_{c3} = 0.79$ ms^{-1}. This air entrainment is subject to hysteresis and by decreasing U, the next critical speed is $U_{c4} = 0.73$ ms^{-1}. Note that by further increasing speed from U_{c3}, instability persists. Continuing to decrease U from U_{c4}, another onset speed is identified at $U_{c5} = 0.28$ ms^{-1}. From this point, the speed must be decreased to just below U_{c1} before the instability subsides. In some cases, the speed coincided with U_{c1}, that is $U_{c6} \leq U_{c1}$.

This pattern is observed for all flow rates 1.7 cm^2 s^{-1} $\leq Q \leq$ 2 cm^2 s^{-1}, i.e. the range of flow rates corresponding to $Q_{\max} < Q < Q_i$.

This pattern of multiple onset-clearance pairs both for increasing and decreasing speed for set flow rates was observed by Clarke (2002) for curtain coating of Newtonian solutions onto roughened substrates. The mechanism for this phenomenon, however, must be qualitatively different given the nature of both the solution (containing surfactant in the current work) and the substrate (pre-wetted as opposed to rough). These results indicate multiple regions of stability/instability for a fixed flow rate. Non-unique speeds for the onset of instability were also reported by Marston et al. (2006b), but the speeds were obtained through a 'path-dependent analysis' varying both substrate speed and flow rate alternately.

The transition between the two regimes (hydrodynamic and flow-field independent) with stable and unstable configurations becoming apparent is unexpected and, as yet, not fully understood. A plausible explanation might be as follows: for $Q < Q_{\max}$, the contact line is downstream of

the rear face of the curtain and as such is dominated by hydrodynamic effects. During this regime, the surfactant and surface age has little or no effect. For $Q_{\max} < Q < Q_i$, initially the contact line is upstream of its optimal location and is subject to surface effects—causing instability at very low speeds (U_{c1}). Upon increasing U, the contact line is brought underneath the curtain and inertial effects stabilise the contact line (U_{c2}). In this region, recirculation at the base of the curtain can occur as indicated by Clarke and Stattersfield (2006). This would lead to an increase in surface age and thus reduction in surface tension. As such, this first clearance boundary might be attributed to the cessation of recirculation at the base of the curtain and subsequent reduction in surface age causing an increase in surface tension, thus stabilising the contact line. From this point, the system will behave as usual in the hydrodynamic regime with instability occurring at U_{c3} and, being subject to hysteresis, will be accompanied by a clearance speed (U_{c4}). Upon further decrease in velocity, surface effects will become more significant once again leading to instability (U_{c5}) which can only be cleared by reduction in speed (U_{c6}). The interaction between the impinging curtain and any residual liquid remaining on the wheel surface (also containing surfactant) will certainly contribute to this unexpected behaviour since the liquid on the surface of the wheel may have relaxed toward the new equilibrium value of surface tension. Indeed, if a $\sigma^{0.77}$ dependence upon the air entrainment speed is assumed [as deduced by Burley and Jolly (1984) for dip coating experiments], which is certain to over-estimate the dependence for the curtain geometry, then a maximum reduction of $\sim 22\%$ is expected for the maximum reduction in surface tension of 26%. In contrast, a threefold reduction has been observed (see Fig. 5). As such, it is clear that the dynamical interaction between the curtain and the residual film is a strong influence. In addition, we note that the estimation of surface tension is likely to be an underestimate since the approximation of surface age from the free-fall time $\sqrt{2h/g}$ will overestimate due to acceleration of the curtain, thus implying an even stronger influence than claimed from the above argument.

This new feature of air entrainment in curtain coating was repeated for both 0.1 and 0.2% concentrations of SDS in a similar viscosity, shown in Figs. 8 and 9. These figures also exhibit the complex hysteresis patterns, again in the very restricted range of flow rates $Q_{\max} < Q < Q_i$.

For the 0.1% SDS solution in Fig. 8, a maximum substrate speed of 1.12 ms^{-1} is attained which is slightly lower than that predicted by Eq. 2 yielding $U_{\max} = 1.25$ ms^{-1}. The flow-field independent velocity $U_i = 0.18$ ms^{-1} is, however, still far below the expected value (0.51 ms^{-1}). This shows that although surface effects are clearly dominant at lower flow rates than expected ($Q_i \approx 2.5$ cm^2s^{-1}),

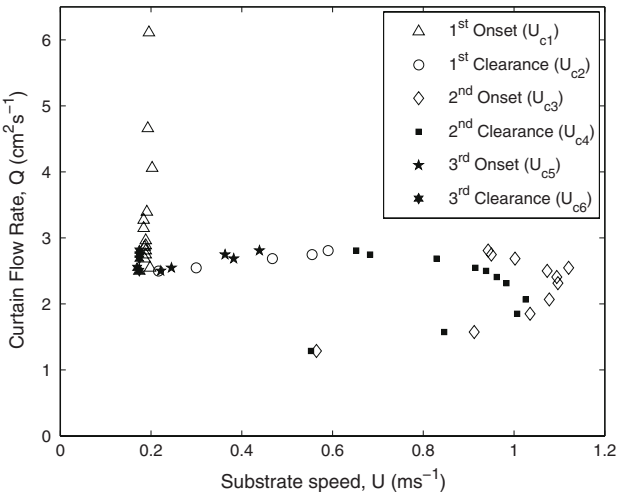

Fig. 8 Onset of air entrainment for a 129 mPa s glycerol solution with 0.1% SDS. $h = 10.7$ cm

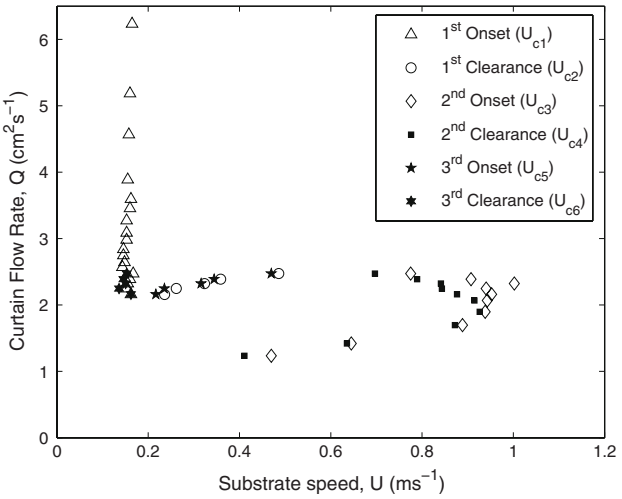

Fig. 9 Onset of air entrainment for a 114 mPa s glycerol solution with 0.2% SDS. $h = 10.7$ cm

the hydrodynamic influence is only marginally reduced at this level of surfactant concentration. In contrast, Fig. 9 shows that at 0.2% concentration, surface effects are becoming substantial throughout the hydrodynamic regime with $U_{\max} = 1$ ms^{-1} showing a 20% reduction from $U_{\max}$ predicted by Eq. 2.

The behaviour reported above in Figs. 5, 6 and 7 was re-examined in a higher viscosity solution (90% glycerol—see Table 1). Figure 10 shows the air entrainment curves for both the surfactant-free and 0.3% SDS cases for a curtain height $h = 2.6$ cm. Here, for the surfactant-free solution, the maximum coating speed attained is $U_{\max} = 0.45$ ms^{-1} (again, in reasonable agreement with Eq. 2 yielding $U_{\max} = 0.49$ ms^{-1}) at $Q_{\max} = 4.23$ cm^2 s^{-1}. The surfactant-filled solution on the other hand shows a significant reduction in both hydrodynamic influence and maximum

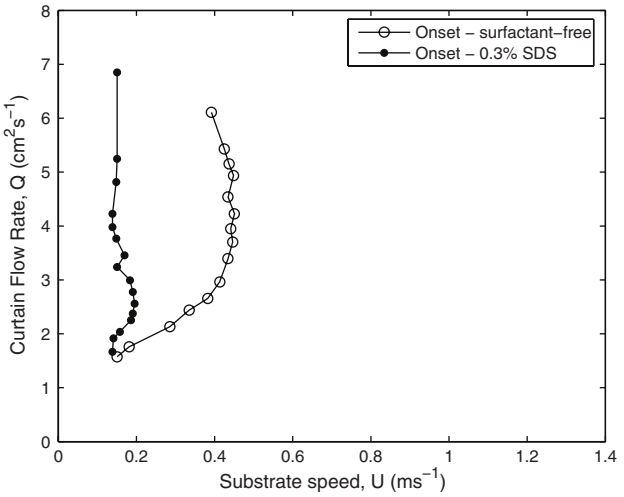

Fig. 10 Onset of air entrainment for surfactant-free ($\mu = 215$ mPa s) and 0.3% SDS ($\mu = 267$) solutions. $h = 2.6$ cm

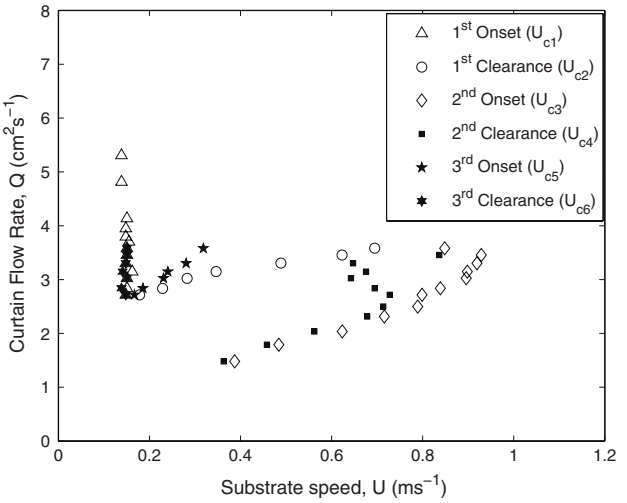

Fig. 12 Air entrainment hysteresis for surfactant-filled solution (0.3% SDS, $\mu = 267$ mPa s). $h = 10.7$ cm

coating speed with $U_{\max} = 0.19$ ms^{-1} at $Q_{\max} = 2.56$ cm^{2}s^{-1} which differs appreciably from that predicted by Eq. 3 ($U_{\max} = 0.44$ ms^{-1}). The behaviour in Fig. 10 is qualitatively similar to that seen in Fig. 5, with a dramatic reduction in both maximum speed and degree of hydrodynamic assist.

In contrast, the hysteresis pattern and multiple onset-clearance data pairs seen only at the highest curtain ($h = 10.7$ cm) for the 85% glycerol solution is now seen at the intermediate curtain height of $h = 6.6$ cm, in Fig. 11. The data for the surfactant-free solution is also given, shown in this plot as filled circles (onset). The new hysteresis pattern, as described previously with three onset-clearance pairs is now; however, only observed in a very restricted range of flow rates, 2.93 cm^2 s^{-1} $< Q <$ 3.12 cm^2 s^{-1}. This indicates a much sharper transition between the hydrodynamic ($Q_{\max}$) and flow-field independent (Q_i) regimes. The maximum coating speed $U_{\max} = 0.48$ ms^{-1} and flow-field independent speed $U_i = 0.14$ ms^{-1} are still below those which would be expected, but not by the same order of magnitude as for the low viscosity solution in Fig. 6.

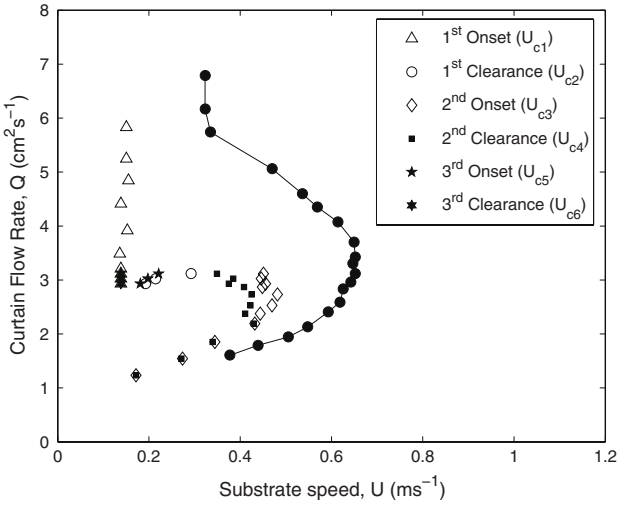

Fig. 11 Air entrainment hysteresis for surfactant-filled solution (0.3% SDS, $\mu = 267$ mPa s) and onset for surfactant-free soltuion ($\mu = 215$ mPa s) shown by solid circles. $h = 6.6$ cm

The equivalent data for the 10.7 cm curtain height is shown in Fig. 12 (for the surfactant-filled solution) and 13 (for the surfactant-free solution). In this case, the hysteresis and multiple onset-clearance data pairs becomes much more obvious and occurs over a larger range of flow rates, 2.7 cm^2 s^{-1} $< Q <$ 3.6 cm^2 s^{-1}. For this fluid, the differences between the usual onset and clearance data points (marked in this instance by U_{c3} and U_{c4}, respectively) become more profound. Note also the divergence between the 'clearance up' (U_{c2}) and 'onset down' (U_{c5}) which is much more substantial than in the previous cases for the low viscosity fluid. In addition to this, a marked increase in maximum speed occurs with $U_{\max} = 0.93$ ms^{-1} exceeding that predicted by Eq. 2 ($U_{\max} = 0.89$ ms^{-1}). This is an indication that the combination of viscosity and inertia are approaching the conditions required for a more intense mode of assist (Blake et al. 2004; Marston et al. 2007a).

The behaviour observed in Figs. 10, 11, 12 and 13 for the higher viscosity fluid is qualitatively similar to that reported in Figs. 6, 7, 8 and 9, showing that the influence of surfactant and the new complex hysteresis is not unique to a single viscosity. It was also seen that the effect becomes more substantial at a higher viscosity where the parameters were approaching those required for a more intense mode of hydrodynamic assist. It is noted, however, that the new hysteresis effect is operating over a narrow range of flow

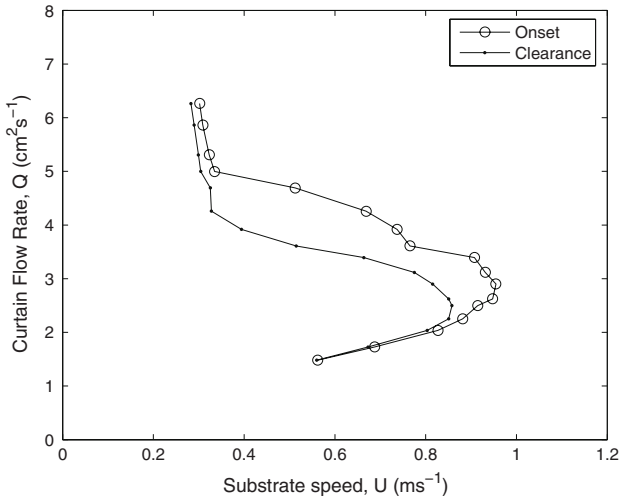

Fig. 13 Onset-clearance of air entrainment for surfactant-free solution ($\mu = 215$ mPa s). $h = 10.7$ cm

rates and elsewhere the behaviour appears qualitatively similar to liquids without surfactant, albeit at significantly lower speeds.

It is expected that this new behaviour will be reproducible over the range of viscosities used in previous publications (Marston et al. 2006a, b, 2007a) but further work, including experiments with dry substrates, will be required to fully understand the physics of this phenomena.

From Figs. 5, 6, 7, 8, 9, 10, 11, 12 and 13 it is clear that the air entrainment phenomena in curtain coating onto pre-wetted surfaces is strongly dependent upon surface tension. Moreover, it is seen that the degree of hydrodynamic assist is also influenced which, together with previous observations (Marston et al. 2006a, b, 2007a), means that hydrodynamic assist is itself a function of viscosity and surface tension. To quantify this is, however, problematic due to restrictions on current technologies for measurement of dynamic surface tension—the subject of continuous research, as discussed by Meissner et al. (2004) and Feinerman and Miller (2004). As such, we take the value measured in 50% glycerol–water mixtures as a first approximation. Regardless of the precise value of surface tension, a new complex feature of instability in curtain coating has been observed which can only be explained by the presence of the the surfactant. The observations made here will need to be repeated for both dry surfaces and higher viscosity liquids to fully understand the role of surfactant in this particular process.

4 Conclusions

An experimental study into the influence of surface tension upon the air entrainment phenomena in curtain coating onto a pre-wet surface has been performed. The addition of small concentrations of surfactant into glycerol–water mixtures significantly reduced the maximum speed at the onset of air entrainment for a given flow rate. In some cases a threefold reduction was observed. The addition of surfactant also reduced the degree of hydrodynamic assist.

Where hydrodynamic effects become substantial, a complex hysteresis pattern emerges which has only been reported previously for rough surfaces. A plausible physical explanation for the observed phenomena was given in terms of the contact line position relative to the curtain. The dynamical interaction of the liquid in the curtain with the residual film, where surface properties may be closer to equilibrium than in the curtain, clearly contributes strongly to this new phenomena.

This new feature of instability in curtain coating appears to become more substantial for increasing inertial effects.

In order to fully quantify the influence of surface tension and the interaction with the residual film, it is recommended that the above experiments be performed for dry substrates.

References

Blake TD, Clarke A, Ruschak KJ (1994) Hydrodynamic assist of dynamic wetting. AIChE J 40(2):229–242

Blake TD, Bracke M, Shikhmurzaev YD (1999) Experimental evidence of nonlocal hydrodynamic influence on the dynamic contact angle. Phys Fluids 11:1995–2007

Blake TD, Dobson RA, Ruschak KJ (2004) Wetting at high capillary numbers. J Colloid Interface Sci 279:198–205

Clarke A (2002) Coating on a rough surface. AIChE J 48:2149–2156

Clarke A, Stattersfield E (2006) Direct evidence supporting nonlocal hydrodynamic influence on the dynamic contact angle. Phys Fluids 18:048106

Cohu O, Benkreira H (1998) Air Entrainment in angled dip coating. Chem Eng Sci 53(3):533–540

Fainerman VB, Miller R (2004) Maximum bubble pressure tensiometry—an analysis of experimental constraints. Adv Colloid Interface Sci 108–109:287–301

Fainerman VB, Makievski AV, Miller R (1993) The measurement of dynamic surface tensions of highly viscous liquids by the maximum bubble pressure method. Colloids Surf A 75:229–235

Fainerman VB, Mys VD, Makievski AV, Miller R (2004) Correction for the aerodynamic resistance and viscosity in maximum bubble pressure tensiometry. Langmuir 20:1721–1723

Lin SP, Roberts G (1981) Waves in a viscous liquid curtain. J Fluid Mech 112:443-458

Marston JO (2008) PhD Thesis, The University of Birmingham

Marston JO, Simmons MJH, Decent SP, Kirk SP (2006a) Influence of the flow field in curtain coating onto a pre-wet substrate. Phys Fluids 18:112102

Marston JO, Decent SP, Simmons MJH (2006b) Hysteresis and non-uniqueness in the speed of onset of instability in curtain coating. J Fluid Mech 569:349–363

Marston JO, Simmons MJH, Decent SP (2007a) Influence of viscosity and impingement speed on intense hydrodynamic assist in curtain coating. Exp Fluids 42(3):483–488

Marston JO, Decent SP, Simmons MJH (2007b) Experimental evidence of non-unique solutions to a steady non-linear coating flow. IMA J Appl Math. doi:10.1093/imamat/hxm062

Meissner J, Kragel J, Frese C, Ruppert S, Fainerman VB, Makievski AV, Miller R (2004) Comparative studies of dynamic surface tensions of $C_{12}EO_6$ solutions measured by different maximum bubble pressure tensiometers. SOFW J 130:41–46

Yamamura M, Suematsu S, Toshihisa K, Adachi K (1999) Experimental investigation of air entrainment in a vertical liquid jet flowing down onto a rotating roll. Chem Eng Sci 55:931–942

Yamamura M, Matsunaga A, Matawari Y, Adachi K, Kage H (2006) Particle-assisted dynamic wetting in a suspension liquid jet impinged onto a moving substrate at different flow rates. Chem Eng Sci 61(16):5421–5426